Peculiar covalent bonding of C 60 / 6H-SiC(0001)-(3 x 3) probed by photoelectron spectroscopy

F.C. Bocquet, L. Giovanelli, Y. Ksari, T Ovramenko, A. Mayne, Gérald Dujardin, F Spillebout, Philippe Sonnet, F Bondino, Elena Magnano, et al.

Peculiar covalent bonding of C_{60}/ 6H-SiC(0001)-(3×3) probed by photoelectron spectroscopy

F.C. Bocquet,[1,2] L. Giovanelli,[3] Y. Ksari,[3] T. Ovramenko,[4] A.J. Mayne,[4] G.Dujardin,[4] F. Spillebout,[5] P. Sonnet,[5] F. Bondino,[6] E. Magnano,[6] and J.-M. Themlin[3]

[1] *Peter Grünberg Institut (PGI-3), Forschungszentrum Jülich, 52425 Jülich, Germany*
[2] *Jülich-Aachen Research Alliance (JARA) – Fundamentals of Future Information Technology, 52425 Jülich, Germany*
[3] *Aix Marseille Univ, University Toulon, CNRS, IM2NP, Marseille 13397, France*
[4] *Univ Paris 11, ISMO CNRS, Institut Sciences Moléculaires Orsay, F-91405 Orsay, France*
[5] *Univ Haute Alsace, CNRS, UMR 7361, IS2M, F-68057 Mulhouse, France*
[6] *IOM-CNR, TASC Laboratory, S.S.14 Km 163,5 Basovizza, 34149 Trieste, Italy*

(Dated: March 18, 2019)

High resolution photoemission with synchrotron radiation was used to study the interface formation of a thin layer of C_{60} on 6$H-$SiC(0001)-(3×3), characterized by protruding Si-tetramers. The results show that C_{60} is chemisorbed by orbital hybridization between the highest-occupied molecular orbital (HOMO) and the p_z orbital of Si adatom at the apex of the tetramers. The covalent nature of the bonding was inferred from core level as well as valence band spectra. The Si 2p spectra reveal that a large fraction (at least 45%) of the Si adatoms remain unbound despite the reactive character of the associated dangling bonds. This is consistent with a model in which each C_{60} is attached to the substrate through a single covalent C_{60}-Si bond. A binding energy shift of the core levels associated with sub-surface Si or C atoms indicates a decrease of the SiC band bending caused by a charge transfer from the C_{60} molecules to the substrate via the formation of donor-like interface states.

I. INTRODUCTION

The adsorption of C_{60} on semiconducting surfaces is a subject of long-standing interest that continues to stimulate the surface science community[1]. Due to its high symmetry and the presence of an extended π-electron system, C_{60} displays many interesting properties. In the solid state, the pristine molecular solid is an insulator that can be turned into a metal and even a superconductor with high transition temperatures when doped with alkali atoms[2]. More recently, using adapted substitutions, C_{60} was proposed as a promising candidate for quantum computing (endofullerenes)[3], drug delivery[4] or H_2 storage[5–9].

For application purposes, C_{60}-derivatives are often transferred on a solid surface, thereby modifying their electronic properties. This is not necessarily a drawback. Depending on the target functionality, one may prefer the C_{60} to retain its single-molecule characteristics or instead to control them by molecule-substrate interaction. The issue of how the C_{60} electronic properties are modified at the C_{60}-semiconductor interface remains a key point for the future development of hybrid molecular devices[10]. Not surprisingly, silicon surfaces were widely employed as a solid support for C_{60}-derivatives. An exhaustive account was published on the subject[11] and a certain agreement exists on the chemisorption character of the *multiple* C_{60}-Si bonds on Si(111)-(7×7) and Si(001)-(2×1). The presence of a possible charge transfer to the molecules has been the subject of much debate. The current understanding is that it is due to the appearance of new interface states rather than the filling of the lowest unoccupied molecular orbital (LUMO)[11].

Silicon carbide (SiC), a wide-bandgap semiconductor with numerous applications in ultra-fast, high power and high temperature electronics[12,13], is an interesting substrate for its peculiar electronic properties. Different surface reconstructions with very contrasting reactivity and corrugation can be obtained under ultra-high vacuum (UHV) by varying the Si/C ratio at the surface[14]. These span from the Si-rich (3×3) to quasi free-standing graphene (QFSG)[15,16], making SiC an interesting playground to study in detail the C_{60}–Si interaction.

In a seminal study of Li et al.[17] devoted to the scanning tunneling microscopy (STM) imagery of fullerenes interacting with Si-rich SiC reconstructions, it was observed that isolated C_{60} adsorb on top of the protrusions which form the (3×3) lattice (since then attributed to adatom-terminated Si tetramers). Annealing the (3×3) covered by 0.02 ML of C_{60} above ∼870 K lead to the decomposition of C_{60}, culminating at ∼1120 K with the formation of ordered SiC islands.

At variance with the later results as well as those for other Si surfaces[18,19] or, more generally, for C_{60} adsorbed on strongly interacting semiconductor surfaces[20], recent spectroscopic studies[21] showed that the molecules adsorbed on the (3×3) do not decompose upon high temperature annealing. Intriguingly, the adsorbed C_{60} desorb above 1140 K so that the (3×3) reconstruction is recovered. This finding is unique among the previously studied Si and Si-rich SiC surfaces. When the bonding is strong and predominantly covalent, C_{60} was always found to dissociate, forming a carbon-rich layer. We attributed this peculiar behavior to the low Si dangling bond (DB) density of the (3×3)

reconstruction and to the highly corrugated character of this adcluster-based reconstruction. Therefore, C_{60} do not decompose at high temperature to form SiC films as claimed by Li et al[17].

The adsorption of C_{60} on the (3×3) reconstruction has also been addressed in a recent study[22], combining STM and density functional theory (DFT). It shows that unlike C_{60}/Si(111)-(7×7) and C_{60}/Si(100)-(2×1), the adsorbed C_{60} can only bind to *a single* reactive Si dangling bond, favoring thermal desorption over molecular decomposition. Moreover, three stable adsorption sites were found by STM with different, though close, adsorption energies as revealed by DFT which take into account van der Waals interactions. This is in contrast with the STM results of Li et al. where only one adsorption configuration was suggested. This site diversity, combined with the mismatch between the lattice parameter (9.27 Å) of the (3×3) reconstruction and the larger intermolecular distance in solid C_{60} (10.01 Å) prevent long range order from developing in the C_{60} monolayer (ML). This implies the presence of a significant fraction of unsaturated Si dangling bonds in the monolayer regime, which should give clear spectroscopic signatures sought in this work. Finally, the calculations indicate that the interface covalent bonding induces a modification of selected C_{60} MOs and predicts a sizable density of states (DOS) at the Fermi level.

The single covalent bond model, proposed on the basis of statistical interpretation of STM images and DFT calculations, still needs to be confronted to spectroscopic data to examine in a quantitative manner several of its consequences. This is the purpose of the present study, which unambiguously confirms the peculiar bonding mechanism at the C_{60}/SiC(0001)-(3×3) interface (using) high-resolution X-ray and UV photoemission spectroscopy (XPS and UPS) with synchrotron radiation to follow the evolution of the valence band (VB) and core level (CL) spectral features as a function of C_{60} coverage. The present work is the first experimental determination of the actual bonding between "as deposited" C_{60} molecules and the (3×3)-SiC substrate. In particular, it avoids the usual recipe to prepare a full monolayer of C_{60} through the mild annealing of a multilayer, which may induce changes in the adsorption configuration[23].

II. METHODS

Synchrotron-light induced XPS and UPS spectra, as well as low-energy electron diffraction (LEED) patterns, were measured at the BACH beamline, Elettra (Trieste). The ultra-high vacuum end-station comprised a preparation and an analysis chamber, both with a base pressure below 5×10^{-10} mbar. The sample was resistively heated, and a flux of silicon atoms was provided by an electron bombarded silicon rod. The sample temperature was measured by an infrared pyrometer using an emissivity of 0.9. We used a SiC sample from a nitrogen-doped (n-type, $N_d = 9 \times 10^{17} cm^{-3}$) $6H$-SiC(0001) wafer by Sterling Semiconductors. The sample was introduced as such in UHV. It was then outgassed at 1250 K for a few minutes and further annealed in a flux of Si atoms to clean the surface. At this stage, a (1×1) pattern was observed in LEED. Annealing the sample at about 1120 K under a higher silicon flux yielded the usual (3×3) reconstruction. The quality of the surface was then assessed by LEED, XPS and UPS spectra. The preparation was repeated until the UPS and XPS spectra were of high quality[24,25], the surface was oxygen-free, and the (3×3) LEED pattern had sharp spots on a low background.

C_{60} was evaporated from a well-degassed Ta crucible heated at 660 K on the sample surface kept at room temperature (RT). The pressure during evaporation was lower than 2×10^{-9} mbar. Samples were obtained by successive depositions. The coverage corresponding to a full monolayer (1 ML) was calibrated by annealing a multilayer sample at 670 K in order to desorb all molecules not in direct contact with the substrate[21,26,27]. Subsequently, sub-ML coverages were obtained by increasing the deposition time on the pristine SiC surface until the C $1s$ spectrum (and the VB) matched that of the ML. Assuming a constant sticking coefficient, sub-ML coverages are proportional to the evaporation duration *i.e.*, 10 min deposition corresponds to about 1 ML, 7 min to about 0.7 ML, etc. Photoemission spectroscopy was performed with a VSW150 electron energy analyzer. All spectra were recorded in normal emission using horizontally polarized light. Si $2p$ core-level was measured with 150 eV photon energy, C $1s$ with 452 eV and VB with 70 eV photon energy. All spectra binding energies (BEs) are referenced to the Fermi level of a gold foil in direct contact with the sample (Au $4f_{7/2}$ BE = 84.0 eV).

III. RESULTS

In this section we present the LEED and photoemission spectra obtained on a clean SiC(0001)-(3×3) and after deposition of increasing quantities of C_{60}. The explored thicknesses are 0.4, 0.7, 1 ML and a multilayer (about 3 ML) referred as thick film (TF).

The LEED patterns for the clean substrate and the two lowest coverages are presented in Fig. 1. The (3×3) diffraction spot intensities gradually decrease with the C_{60} coverage. No intensity from the underlying (3×3) could be observed for the 1 ML and TF samples. Moreover, no new spots arising from the C_{60} overlayer could be observed

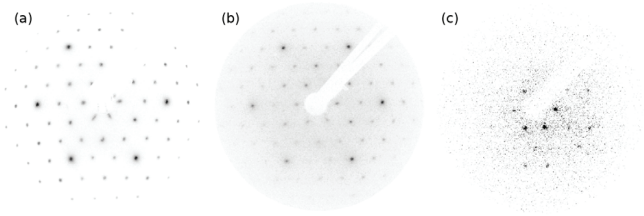

FIG. 1: LEED patterns of (a) clean SiC(0001)-(3 × 3) (E_P=101 eV), (b) 0.4 ML of C_{60} on (3 × 3) (E_P=101 eV) and (c) 0.7 ML of C_{60} on (3 × 3) (E_P=85 eV). The ML and the TF yielded no detectable pattern.

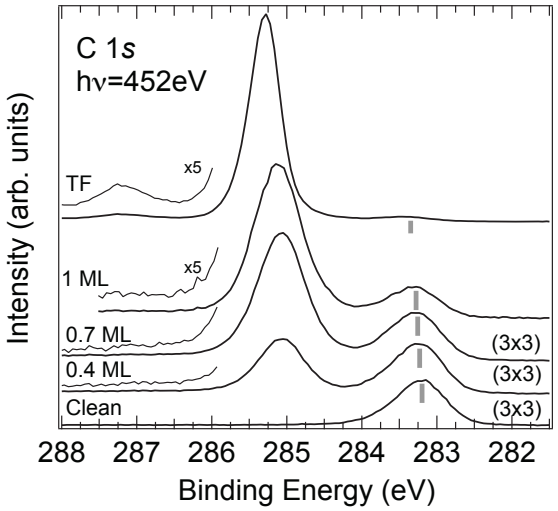

FIG. 2: C 1s CL measured with $h\nu = 452$ eV in normal emission for the clean SiC(0001)-(3 × 3) substrate and as a function of C_{60} coverage. The sample coverage and the observed LEED pattern, if any, are indicated. The high and low BE peaks are due to adsorbed C_{60} and to sub-surface SiC carbon atoms, respectively. The gray vertical bars indicate the SiC peak positions for each coverage.

for any of the studied samples, confirming that at the interface with SiC(0001)-(3 × 3) the molecules adsorb without long range order[21,22].

The C 1s spectra measured in normal emission for different C_{60} coverages are shown in Fig. 2. The C 1s spectrum of the clean (3 × 3) reconstruction shows a single, symmetric peak at about 283.2 eV due to the bulk C atoms of the SiC substrate, in agreement with previous results[28]. After molecular deposition the SiC bulk feature loses intensity and simultaneously another peak attributed to C_{60} grows at a BE of about 285 eV. Its full-width at half-maximum (FWHM) is 0.75 eV up to 1 ML and decreases to 0.55 eV for the TF. A shake-up satellite appears around 287 eV for the TF sample only, as shown by the magnified data. As coverage increases, the spectra shift to higher BEs. This is highlighted for the substrate component by gray vertical bars.

Fig. 3 displays the Si 2p CLs. Since the amount of silicon atoms at the surface is likely to remain constant during C_{60} deposition, we chose to normalize the data to their total area after removing an integral background. This procedure compensates for the attenuation due to the increasing C_{60} coverage and eases the comparison. The clean (3 × 3) spectrum clearly results from the addition of several spin-orbit doublets[24]. A precise assignment will be given in the next section but for the moment it can be noticed that two clear maxima at 100.2 and 99.5 eV BE are visible, as well as shoulders on the higher and lower BE sides. As the C_{60} coverage increases, the spectral features are less defined. This broadening is due to the molecule-substrate interaction. Nevertheless, a progressive shift to higher BE is observed as highlighted by the gray vertical bars positioned on the main features as a guide to the eye. The shift of each component composing the spectra will be analyzed in the next section. Finally, the TF and the ML spectra are almost identical, testifying that second layer molecules do not interact appreciably with the substrate.

The VB spectra are presented in Fig. 4. The spectrum of the clean (3 × 3) substrate displays two surface states in the SiC bulk band gap[29] at BEs of 0.6 eV (S_1, a Mott-Hubbard state[30,31]) and 1.5 eV (S_2) followed by high intensity features at 3 and 6 eV. The VB spectrum of the C_{60} TF is similar to that reported in the literature[18]. By comparing

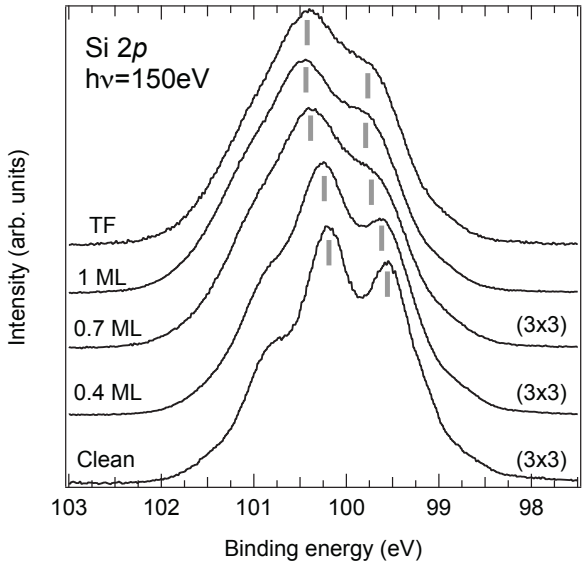

FIG. 3: Si 2p CL measured at $h\nu = 150$ eV in normal emission for the clean SiC(0001)-(3 × 3) substrate and as a function of C_{60} coverage. The intensity of each spectrum is normalized so to have a constant area. The gray vertical bars indicate the evolution with coverage of two of the peak positions.

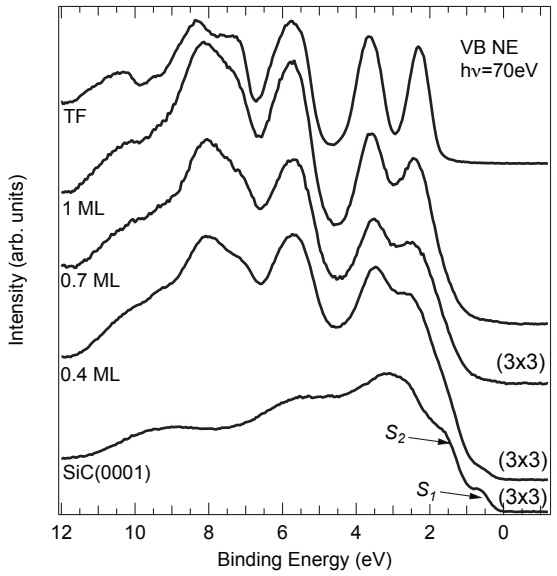

FIG. 4: VB measured at $h\nu = 70$ eV, in normal emission for the clean SiC(0001)(3 × 3) substrate and as a function of C_{60} coverage.

the valley depth between the highest-occupied molecular orbital (HOMO) and the HOMO-1 to previous studies of C_{60} on semiconductors,[18,32] we estimate a thickness of about 3 ML for the TF. Upon adsorption of C_{60}, the SiC features gradually decrease at the expense of the C_{60} VB. At the same time and as for the CLs, the VB shifts to higher BE as coverage is increased. We notice that the SiC peak around 3 eV lies in between the HOMO and HOMO-1 peaks thus preventing a clear assignment of line shape modification of the molecular states. In the next section, an attempt is made to overcome this difficulty by a background subtraction procedure. At higher BE the substrate contribution is less important and one can confidently state that the feature at 6 eV looks unchanged whereas the one centered at 8 eV shows a clear modification upon adsorption. Finally, as found for other C_{60}-Si interfaces,[18,33] no clear C_{60}-related peak at the Fermi level is detected in the present case of C_{60}/SiC(0001)-(3 × 3) for any coverage considered here.

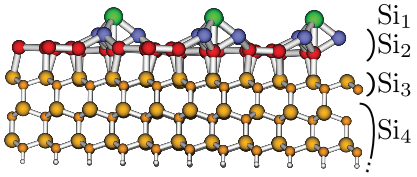

FIG. 5: (color online) Ball and stick representation of the (3×3) reconstruction, showing Si-tetramers with one Si at their apex (Si-adatom in the text). Silicon and carbon atoms are represented by large and small sphere respectively. The set of silicon atoms participating in each core level component used in the fitting procedure is indicated along with the component label.

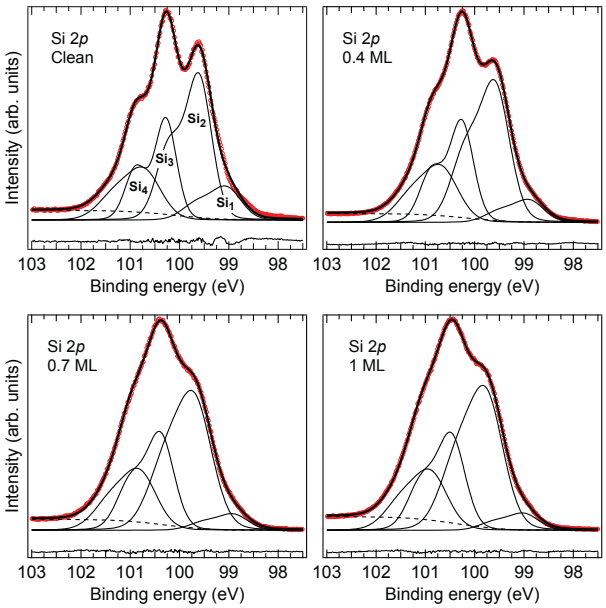

FIG. 6: (color online) Experimental points (red circles) and fit (thick line) of Si $2p$ CLs measured with $h\nu = 150$ eV. The fit residuals are shown below each spectrum. The four components are shown with a thin line. The dashed line is the integral background.

IV. DISCUSSION

A. Spectra analysis : Si $2p$ core levels

To extract more information from the analysis of the CLs, a systematic fitting procedure has been performed on both the substrate and adsorbate spectra. Virojanadara *et al.* showed that at least four components are necessary to fit the Si $2p$ CL spectrum of the Si(0001)-(3×3) surface, each component being associated with a given atomic site within the reconstruction[24]. A side view of the accepted structural model of the (3×3) is shown in Fig. 5. It is composed of a twisted adlayer of silicon terminating the bulk SiC crystal and covered by silicon tetramers. Following Ref.[24], we fitted the clean SiC(0001)-(3×3) spectrum with four Voigt components with a spin-orbit splitting of 0.61 eV and a branching ratio of 0.51 (Fig. 6). In the Si $2p$ spectrum of the clean substrate, the most intense component (Si_2) is due to Si atoms of the Si adlayer together with the atoms at the base of the tetramers. At lower BE a component (Si_1) is necessary to fit the data: it is assigned to the Si adatoms at the vertex of the tetramers (Si-adatoms). Their lower BE is due to the reduced coordination and to the presence of a dangling bond at the origin of the Mott-Hubbard surface states[34]. Si_3 and Si_4 are due to atoms lying further away from the surface: Si atoms from the last Si-C bilayer and to bulk Si atoms, respectively.

C_{60} adsorb on SiC(0001)-(3×3) through covalent bonds with silicon adatoms[22]. Accordingly the Si_1 component decreases as coverage is increased in the sub-ML range. At the same time a new component (accounting for the Si atoms now bound with C_{60}) should appear at about 0.9 eV higher BE[33,35]. Nevertheless, since such component falls in the energy range of the intense Si_2, including a fifth component in the fitting procedure is not reasonable. In order

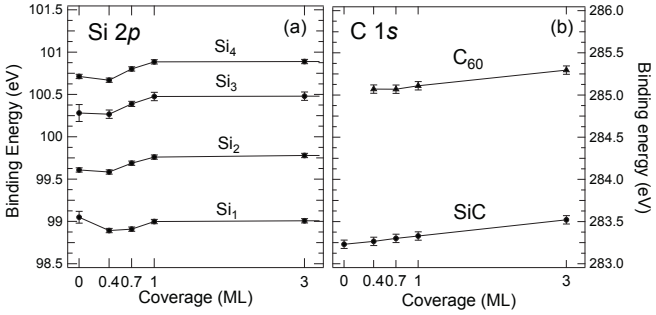

FIG. 7: Fit results of the Si $2p$ and C $1s$ CLs as a function of coverage. The left panel (a) displays the Si $2p_{3/2}$ BE of the different components of the Si $2p$ spectra (see Fig. 6). In the right panel (b) the BE of the C $1s$ spectra of the C_{60} and sub-surface SiC are reported. Note that the energy range spanned is the same in the two panels.

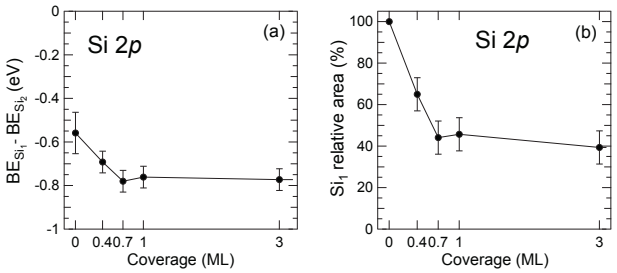

FIG. 8: Fit results of the Si $2p$ CLs measured in normal emission as a function of coverage. (a) BE difference between the Si_1 and the Si_2 component; (b) area of the Si_1 component relatively to its value in the spectrum of the clean SiC(0001).

to account for its presence we have considered the Si_2 FWHM as a free parameter keeping the FWHM of the other components fixed. Such a procedure is justified by the fact that the atoms in the sub-surface region (i.e. Si_3 and Si_4) are only marginally affected by a chemical modification at the surface since they are excluded from any direct bonding with the adsorbates. This observation leads to a further constraint on the fit, that is a constant area ratio between Si_4 and Si_3. The relative energy of each component was in accordance with the literature results on the clean (3×3)[24]. From Fig. 6, it can be seen that the fit residuals of the clean sample are not entirely satisfactory on the low BE side[74]. Such feature is probably ascribable to the presence of low-coordination atoms at surface defects (around 5 - 10 % on SiC(0001)-(3×3)[22]) and to the small terrace size leading to Si atoms at step edges[36–40].

By comparing the different spectra, it is clear that the Si_1 component is reduced upon molecular adsorption while, simultaneously, the FWHM of the Si_2 gradually increases. Least-square fitting gives a 35 % FWHM increase up to 0.7 ML where it stabilizes up to the highest nominal coverage of 1 ML. This can be ascribed to the bonding of the C_{60} with the substrate tetramer-Si apex adatoms as explained above. Nevertheless, the adatom component is not entirely suppressed as discussed in detail below.

Previous studies on Si(111) and Si(100) showed that Si-C bond formation upon C_{60} adsorption promotes a positive BE shift of the Si $2p$ related components[33,35]. The trends and behavior of the different components have been estimated from the BEs and intensities used to fit the spectra; they are summarized in Fig. 7 and 8. It is then possible to appreciate that components Si_2, Si_3 and Si_4 all shift to higher BE as the coverage increases (Fig. 7.a), reflecting the trend previously observed in Fig. 3. Simultaneously, the fitting of the C $1s$ (Fig. 7.b) highlights a similar behavior for the C substrate atoms. This concomitant shift is likely to result from a charge transfer affecting the entire space-charge layer region and may be attributed to a decrease of the substrate band-bending induced by the C_{60} adsorption (see next section). However, the Si_1 component does not follow the parallel shift of the other components of Si $2p$ CLs. Interestingly, when comparing their BE with that of Si_2 (identical results are obtained with Si_3 or Si_4 as references), a decrease of BE is observed (see Fig. 8-a) when the coverage approaches 1 ML. This can be understood considering that, at variance with other non-C_{60}-bound sites, Si_1 adatoms lie very close to the adsorbed molecules and thus experience a more effective photo-hole screening in the final state, reducing their BE[41].

We now go back to the intensity reduction of the Si_1 component initially observed in Fig. 6 and attributed mainly to the hybridization of the dangling bonds localized on Si adatoms with C_{60} molecular states. Using DFT calculations

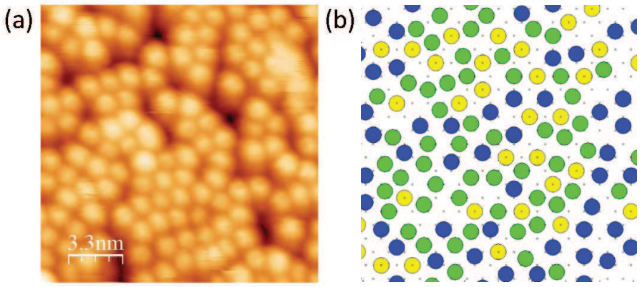

FIG. 9: (color online) (a) STM image (left panel, V_Pol=-4V, I=0.3nA) *vs* (b) hard sphere model (right panel) of the pseudo-compact and disordered C_{60} monolayer adsorbed on SiC(0001)-(3×3). The hexagonal lattice (black crosses) represents the Si-adatoms on top of the Si-tetramers, while the large colored circles are mimicking the C_{60} molecules adsorbed on three types of sites: on-top a Si-tetramer (yellow disks), between two Si-tetramers (green disks) or between three Si-tetramers (blue disks) (see text for details).

and adopting a simple structural model involving three stable adsorption sites, it was recently proposed[22] that every C_{60} is covalently bound to *a single* Si adatom, even when the C_{60} is positioned in between two or three tetramers, the latter being the most stable configuration. The Si_1 *relative* area evolution (see Fig. 8-b) shows that a significant fraction of the Si DB remain unaffected by interface hybridization. Indeed, the Si_1 intensity diminishes up to one ML and then remains constant at about 45%± 5% of its initial value (100%). Since some of the Si_1 intensity is probably attenuated by the adsorbed C_{60}, we take 0.4 as a lower limit to the fraction of *unreacted* Si tetramers. As mentioned in the introduction, due to the difference in the (3×3) lattice parameter and the larger intermolecular distance in solid C_{60}, a significant fraction of Si adatoms can not bind to a C_{60}. Furthermore, the existence of three stable adsorption sites leads to a disordered C_{60} 1 ML on top of the SiC(0001)-(3×3) reconstruction[22].

Since the present data give an estimation of the remaining DB fraction at ∼1 ML coverage, it is interesting to compare this value with the single covalent bond model proposed in Ref.[22]. For this, we modeled an adsorbed C_{60} monolayer using hard spheres mimicking C_{60}, randomly placed (at the same height) on a checkerboard made of an hexagonal 2D lattice (lattice parameter of 9.27 Å) representing the reactive Si-tetramers. The latter defines three types of hosting sites, mimicking in turn the three types of adsorption sites of the single covalent bond model (*e.g.* on-top a Si-tetramer, between two or between three Si-tetramers). Fig. 9.b shows one possible outcome of this stochastic simulation, with a mixture of hard spheres randomly placed at the three sites (roughly equipopulated). We imposed a minimum distance between first neighbours larger than 10.7 Å, so that neighboring spheres can not share any tetramer[75]. From this crude model, we estimate the relative concentration of covalently bound Si-adatoms by counting a single C_{60}-Si bond per molecule whatever the adsorption site. The picture of Fig. 9.b shows a relatively open structure with a ratio of 66 ± 5% of unreacted Si-adatoms, to be compared with the experimental result (45 ± 5%), the difference being attributed to the selective attenuation of the photoelectrons from the Si_1 component by the buckyballs. Finally, in Fig. 9, an STM image of this interface close to ∼1 ML coverage[76] is compared to the model.

B. Charge transfer mechanism

In the following, we address the origin of the band bending modifications described above. In this perspective, some aspects of the C_{60}–SiC interface will be recalled briefly. The aim is to show that (i) the initial space-charge layer of the (3×3) is (for n-type samples) a depletion layer with a positive (upwards) surface band bending of around 1.2 eV, and (ii) that C_{60} adsorption induces a reduction of this band bending resulting from the formation of *donor-like* interface states whose origin will be discussed.

The initial band bending of the (3×3) reconstruction can be evaluated through our previous studies of the 6*H*-SiC surfaces and graphene/SiC interfaces which show characteristic bulk-derived features in inverse photoemission spectroscopy (IPES)[14,21,42]. In fact, the normal incidence IPES spectra of 6*H*-SiC reconstructions all exhibit a prominent peak around 7 eV above E_F, derived from SiC unoccupied bulk states[43,44]. Owing to the high surface sensitivity of IPES, this bulk-derived feature can be used for probing the band bending variations of the substrate. Since this SiC-derived peak appears at about the same position for the (3×3), $(\sqrt{3} \times \sqrt{3})$ and QFSG layer, we estimate that the initial space-charge layer of the (3×3) reconstruction is close to the $(\sqrt{3} \times \sqrt{3})$[14] and the QFSG[44], *i.e.* a charge depletion layer (for n-type samples) resulting in a large, positive (upwards) band bending. In the framework of the polarization model[45,46], this peculiar depletion layer has been assigned to the spontaneous polarization of the

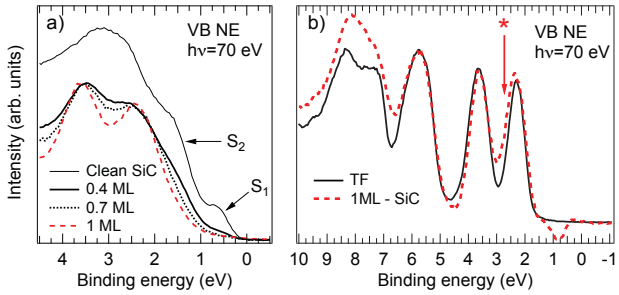

FIG. 10: (color online) (a) Comparison of the low BE part of the VB spectra for the clean SiC(0001)-(3 × 3) and up to 1 ML C_{60} coverage; (b) comparison of the thick layer VB spectrum (thick line) and the 1 ML spectrum (dashed line) after substrate background subtraction. The vertical arrow indicates the broadening of the HOMO for the ML spectrum.

pyroelectric hexagonal SiC substrate, which induces a negative pseudo polarization charge at the SiC surface. For n-doped ($N_D = 5.0 \times 10^{17} cm^{-3}$) 6*H*-SiC samples covered by a QFSG, the surface band bending has been estimated to ~ 1.2 eV[46] and we take this value as an estimation of the initial upward band bending of the (3×3) reconstruction.

We argue that the formation of a chemical bond between C_{60} and the (3×3) adatoms promotes a partial positive charge localized on the molecule. Indeed, as recalled in Ref.[22], when an electron from a Si dangling bond combines with an electron from a p_z orbital of one of the C_{60} carbon atoms to form a covalent Si-C bond, this electron is removed from the π-electron system of C_{60} which then acquires an effective partial positive charge. Acting as surface-localized donors, adsorbed fullerenes thus induce a positive surface charge density variation ΔQ_{ss}, which is compensated by a negative space charge variation ΔQ_{sc} and a concomitant decrease of the initial SiC band bending. The average CL shift from substrate Si atoms (Fig. 7) gives a band bending reduction of about $\sim 0.15 \pm 0.1$ eV.

It is interesting to compare the picture sketched above with previous results for other semiconductor surfaces. For the well-known reconstructions of Si(111), the presence of charged electronic surface states and the reduced band gap at the surface[77] are usually associated with some degree of Fermi level pinning[47], suppressing or reducing the amplitude of any band bending variation upon sub-ML adsorption. More generally, the degree of Fermi level pinning at a given surface depends on the peculiarities of its electronic structure. In this context, the existence of a metallic surface able to pin the Fermi level is an exception rather than a rule[47]. In most cases, upon adsorption, the Fermi level is free to move throughout the surface electronic band gap, determined by the position of the filled and unfilled electronic states. For instance, upon C_{60} adsorption on the basal (001) face of GeS[48], the Fermi level can move within the band gap of GeS(001) due to the lack of intrinsic surface states associated with its layered structure. For the surfaces of III-V semiconductor compounds, a variety of reconstructions generally induce a sizable surface band gap[47] and an unpinned Fermi level. In turn, this allows significant band bending variations to compensate the appearance of a surface electrical charge density Q_{ss} following sub-ML adsorption of foreign species (see *e.g.* Ref.[49]).

Band bending variations through substrate CL shifts observed upon adsorption of C_{60} on semiconductor surfaces are thus often used as a fingerprint of charge transfer at the interface. For instance, for *n*-type GaAs(110)[50] a charge transfer of 0.02 substrate electrons for each C_{60} causes a shift of the substrate CLs to lower BE by 0.3 eV. Similarly, for C_{60} adsorption on *n*-doped GeS(001)[51], a BE shift of 0.2 eV in the opposite direction was interpreted as charge delocalization of a fractional amount of C_{60} electrons to the substrate space charge layer. Other studies on different low-reactivity substrates report similar behaviors[11,52,53]. Such a scenario likely holds for fullerene adsorption on the Mott-Hubbard insulator SiC(0001)-(3 × 3) reconstruction, due to its significant surface band gap ($\gtrsim$1 eV) which separates the fully occupied one-electron S_1 surface state from its unoccupied counterpart U_1[34]. In the present case of C_{60}/SiC(0001)-(3 × 3), the reduction of the upwards band-bending towards flat bands is indicative of a charge transfer from the molecule to the substrate. This charge transfer is facilitated by the initial depletion layer of the SiC substrate, which corresponds to an upwards bending of the valence and conduction bands by $\sim$1.2 eV and an increased work function *w.r.t.* flat bands.

C. Valence band

The valence band spectra measured by UPS give a clearer picture of the evolution of the surface states and the changes to the molecular orbital upon adsorption. In Fig. 10.a an enlargment of the VB in the low BE region is shown. At 0.4 ML coverage, although strongly attenuated, the two surface states are still visible. For higher coverage they

gradually diminish and at 1 ML they are no longer detectable. This observation does not contradict our conclusions, based on the Si 2*p*, that a significant fraction of silicon adatoms are not hybridized with the molecules. Indeed, it is known that Mott-Hubbard states (S_1 and U_1) are collective electronic states that develop through nearest-neighbor interactions. Interestingly, although more than 45% of the Si adatoms remain unhybridized with the molecules, this is sufficient to quench the collective surface and Mott-Hubbard states.

In order to highlight the modifications occurring to the C_{60} MOs upon adsorption, we display in Fig. 10.b the 1 ML and the TF spectra after a substrate background subtraction and BE shift to align the HOMO BEs. Moreover, in the low BE region, the intensity is scaled such that the HOMO and HOMO-1 intensities are equal for the two systems whereas above 4.5 eV the normalization is made on the strong feature around 6 eV. It can be seen that the HOMO-1 is virtually unaffected by the interaction whereas a clear broadening is observed for the HOMO[78] (particularly on the high BE side as indicated by a vertical arrow). This is in perfect agreement with DFT-calculated interface DOS[22] where a C_{60}-Si adatom covalent interaction was inferred, showing an unchanged HOMO-1 and a small splitting of the HOMO with the appearance of a shoulder on the high BE side. Similarly, C_{60}-Si multi-bond formation for C_{60}/Si(111)-(7×7) and C_{60}/Si(100)-(2×1) also show a broadening of the HOMO associated with the formation of C-Si σ-bonds[54,55]. The broadening of the HOMO in the UPS VB on those systems was explained by the splitting of the HOMO in two components separated by 0.5 eV[56,57]. Comparatively, in the present case the HOMO splitting has a slightly smaller value of 0.4 eV (data fit not shown).

HOMO hybridization is not the only C_{60} VB modification predicted by DFT for this system. In Ref.[22] it was suggested that the partial positive charge localized on the adsorbed C_{60} may be compensated, to some extent, by an electron transfer from the substrate. Such a charge transfer towards the molecule was previously predicted as well for C_{60}/Si(111)[11,54,58] and C_{60}/Si(100)[11,55,59] interfaces, where each molecule is engaged in multiple C_{60}-Si bonds. For C_{60}/SiC(0001)-(3×3) the calculated charge transfer appears in the VB through the presence of a DOS crossing the Fermi level, largely delocalized on the C_{60} molecules[22]. Even though a small intensity is indeed present in the vicinity of the Fermi level, the present data (in line with UPS studies on C_{60}/ Si(111) and Si(100)[11]) do not allow a clear assignment of this feature to an interface charge transfer. The DFT simulations might not describe very well the position of the electronic interface states, which may be affected *e.g.* by strong correlation effects. The present results are then consistent with donor-like interface states localized above the Fermi level.

At higher BE two strong features produced by σ states dominate the spectra. The peak at about 6 eV is essentially unchanged upon adsorption whereas the one centered at 8 eV shows some changes, indicating that a substantial electronic redistribution affects some selected σ states of the adsorbed C_{60} following hybridization.

D. C 1*s* core level

The C 1*s* CL spectra (Fig. 2) present two peaks which can be fitted by two symmetric components. The BE values resulting from the fit are shown in Fig. 7.b. The substrate CL shift has already been addressed in the earlier discussion of the band bending reduction. Concerning the C 1*s* of C_{60} a very similar shift is found suggesting that the effect of interface bonding is negligible here.

As mentioned in Section III (see Fig. 2) the molecule-substrate interaction causes a line shape broadening of the C 1*s* spectrum between the TF and the ML (and sub-ML). The C_{60} C 1*s* FWHM is 0.55 eV for the former and 0.75 eV for the latter, respectively. The line shape of the C 1*s* spectrum is a powerful tool to probe the chemical modifications of adsorbed C_{60} molecules. In the gas phase all the atoms in the molecule are equivalent and the spectrum displays a narrow symmetric peak[60,61]. In the molecular solid or for physisorbed molecules the C_{60} atoms are no longer equivalent although hardly seen in the spectrum[62]. Strongly broadened and asymmetric spectra are instead observed as a result of charge transfer to the molecules adsorbed on metallic substrates[63–65]. Such modifications of the C 1*s* spectrum are due to final state screening by the electronic excitations at the interface. The C atoms within an adsorbed C_{60} are then strongly inequivalent because of their different distances from the substrate[65]. On the other hand, even when the C_{60}-substrate interaction is strong (as proved for instance by the VB spectra or the desorption temperature), a covalent bond at the interface results in narrow C 1*s* spectra[65–67]. The bonding character (*i.e.* ionic vs. covalent) can then be determined from the line shape analysis.

When C_{60} is deposited on Si single-crystal surfaces the formation of C_{60}-Si hybrid states is generally favorable as inferred from the HOMO splitting in UPS spectra[18,33,56]. DFT calculations suggested that interface bonding is indeed due to a covalent bond formation with some charge transfer to the C_{60} molecules. At variance with what was found on metal surfaces, such charge transfer is not due to partial LUMO filling but rather to HOMO hybridization with Si dangling bonds[54,55]. As a consequence the C 1*s* main component is broadened by the interaction but still appears rather narrow and symmetric[33,68] if compared to C_{60} on metal charge-transfer systems involving LUMO filling. The line shape found here for C_{60}/SiC(0001)-(3×3) is basically the same as that found for C_{60}/Si(111)-(7×7), confirming a strong, predominantly covalent chemisorption picture[69]. Such a scenario is further supported by the disappearance

of the shake-up satellite at $\sim$ 1.9 eV higher BE from the main C_{60} peak upon adsorption (see magnified inset in Fig. 2). The shake-up feature is due to the final-state system relaxation following core-hole creation which allows low-energy electronic excitations (namely the low-lying HOMO-LUMO transition). The shape and intensity of such a feature is very sensitive to the interface bonding[65,67,69,70]. The fact that in the present case the shake-up satellite is completely washed out testifies to a sizable interface interaction.

V. CONCLUSIONS

Using core-level and valence band photoemission, we studied the adsorption of C_{60} on SiC(0001)-(3×3) in the sub-ML up to a full monolayer and beyond. Valence band spectra show that the C_{60} HOMO state is affected by the interaction, confirming that this MO hybridizes with substrate states through a covalent C_{60}-Si bonding. This is also confirmed by the lineshape broadening of the C $1s$ at the interface, similar to that observed for C_{60}/Si(111) for which the HOMO splitting upon bonding was indeed more accentuated. The analysis of the high-resolution Si $2p$ core-level spectra shows that around $\sim 1ML$ C_{60}, a large fraction (more than $\sim$ 45%) of the tetramer-Si dangling bonds are left unreacted despite their reactive character.

These findings appear fully consistent with the single covalent bond model proposed by Ovramenko *et al.* on the basis of the statistical analysis of STM image and DFT calculations, which considers the C_{60} adsorption on three types of sites with a single covalent bond per C_{60}. Therefore, the C_{60} adsorbed on top of or between two or three Si-tetramer form a disordered, pseudo-compact first monolayer with a relatively open structure consistent with the STM images, well reproduced here by a stochastic model.

In the valence band, the low concentration of reacted dangling bonds appears sufficient to destroy the collective Mott-Hubbard surface state, since the associated peak in the valence band appears already quenched around 0.7ML. Furthermore, in contrast to the DFT-calculation predictions, our UPS spectra do not reveal any appreciable change of the density-of-states in the vicinity of the Fermi level.

Using substrate and adsorbate core level shifts, we show that the initial upward band bending of SiC is partially removed. We explain this effect by a charge transfer from the C_{60} molecules to the SiC substrate following the formation of a single covalent C-Si bond per C_{60} resulting in unoccupied (donor-like) interface states. The C_{60}-SiC bond has thus some ionic character, but in strong contrast with the predictions of DFT-calculations, there is a charge transfer from the C_{60} to the substrate.

These findings shed a new light on the physics and chemistry of fullerene adsorbed on the (3×3) reconstruction of SiC(0001). Indeed, other large, planar and pi-conjugated molecules are known to link to the SiC(0001)(3×3) through *a pair* of Si tetramers to keep the pi-conjugation throughout the molecule[71,72]. The single covalent bond model also explains why, in contrast to other Si surfaces, this system shows an unexpected high temperature desorption of the C_{60} while leaving a clean reconstruction[21]. Extended and regular array of molecules attached on top of nano-protrusions by a strong, single covalent bond while keeping the possibility of thermal desorption could prove useful in order to localize endohedral magnetic fullerenes[3,73] on a surface with a minimum perturbation of the molecular cage orbitals, or to produce a rectifying molecular monolayer through the use of heterofullerenes[10].

Acknowledgments

This work was supported by the ANR PNANO project MolSiC (ANR-08-P058-36).

[1] G. Otero, G. Biddau, C. Sánchez-Sánchez, R. Caillard, M. F. López, C. Rogero, F. J. Palomares, N. Cabello, M. A. Basanta, J. Ortega, et al., Nature **454**, 865 (2008), ISSN 0028-0836, URL `http://www.nature.com.lama.univ-amu.fr/nature/journal/v454/n7206/full/nature07193.html`.

[2] O. Gunnarsson, Rev. Mod. Phys. **69**, 575 (1997).

[3] W. Scherer and M. Mehring, The Journal of Chemical Physics **128**, 052305 (pages 11) (2008), URL `http://link.aip.org/link/?JCP/128/052305/1`.

[4] J. M. Ashcroft, D. A. Tsyboulski, K. B. Hartman, T. Y. Zakharian, J. W. Marks, R. B. Weisman, M. G. Rosenblum, and L. J. Wilson, Chem. Commun. pp. 3004–3006 (2006), ISSN 1359-7345.

[5] Y. Zhao, Y.-H. Kim, A. C. Dillon, M. J. Heben, and S. B. Zhang, Phys. Rev. Lett. **94**, 155504 (pages 4) (2005), URL `http://link.aps.org/abstract/PRL/v94/e155504`.

[6] Y. Yamada, Y. Satake, K. Watanabe, Y. Yokoyama, R. Okada, and M. Sasaki, Phys. Rev. B **84**, 235425 (2011), URL `http://link.aps.org/doi/10.1103/PhysRevB.84.235425`.

[7] J. A. Teprovich, M. S. Wellons, R. Lascola, S.-J. Hwang, P. A. Ward, R. N. Compton, and R. Zidan, Nano Lett. **12**, 582 (2011), ISSN 1530-6984, URL http://dx.doi.org/10.1021/nl203045v.

[8] Q. Wang and P. Jena, J. Phys. Chem. Lett. **3**, 1084 (2012), ISSN 1948-7185, URL http://dx.doi.org/10.1021/jz3002037.

[9] A. Kaiser, C. Leidlmair, P. Bartl, S. Zöttl, S. Denifl, A. Mauracher, M. Probst, P. Scheier, and O. Echt, J. Chem. Phys. **138**, 074311 (2013), ISSN 00219606, URL http://jcp.aip.org/resource/1/jcpsa6/v138/i7/p074311_s1.

[10] J. Zhao, C. Zeng, X. Cheng, K. Wang, G. Wang, J. Yang, J. G. Hou, and Q. Zhu, Phys. Rev. Lett. **95**, 045502 (2005).

[11] P. J. Moriarty, Surf. Sci. Rep. **65**, 175 (2010), ISSN 0167-5729, URL http://www.sciencedirect.com/science/article/B6TVY-5133HW7-2/2/400545167ea69e56fc104040edd40ed1.

[12] D. Nakamura, I. Gunjishima, S. Yamaguchi, T. Ito, A. Okamoto, H. Kondo, S. Onda, and K. Takatori, Nature **430**, 1009 (2004), ISSN 0028-0836, URL http://www.nature.com/nature/journal/v430/n7003/full/nature02810.html.

[13] H. Okumura, J. J. Appl. Phys. **45**, 7565 (2006), URL http://jjap.jsap.jp/link?JJAP/45/7565/.

[14] I. Forbeaux, J.-M. Themlin, and J.-M. Debever, Phys. Rev. B **58**, 16396 (1998).

[15] C. Riedl, C. Coletti, T. Iwasaki, A. A. Zakharov, and U. Starke, Phys. Rev. Lett. **103**, 246804 (2009).

[16] F. C. Bocquet, R. Bisson, J.-M. Themlin, J.-M. Layet, and T. Angot, J. Phys. D **47**, 094014 (2014), ISSN 0022-3727.

[17] L. Li, Y. Hasegawa, H. Shinohara, and T. Sakurai, J. Vac. Sci. Technol. B **15**, 1300 (1997), URL http://link.aip.org/link/?JVB/15/1300/1.

[18] C. Cepek, P. Schiavuta, M. Sancrotti, and M. Pedio, Phys. Rev. B **60**, 2068 (1999).

[19] A. Hamza and M. Balooch, Chemical Physics Letters **201**, 404 (1993), ISSN 0009-2614, URL http://www.sciencedirect.com/science/article/pii/0009261493850923.

[20] G. Bertoni, C. Cepek, and M. Sancrotti, Appl. Surf. Sci. **212-213**, 52 (2003), ISSN 0169-4332, 11th International Conference on Solid Films and Surfaces, URL http://www.sciencedirect.com/science/article/pii/S0169433203000254.

[21] F. C. Bocquet, Y. Ksari, L. Giovanelli, L. Porte, and J.-M. Themlin, Phys. Rev. B **84**, 075333 (2011).

[22] T. Ovramenko, F. Spillebout, F. C. Bocquet, A. J. Mayne, G. Dujardin, P. Sonnet, L. Stauffer, Y. Ksari, and J.-M. Themlin, Phys. Rev. B **87**, 155421 (2013), URL http://link.aps.org/doi/10.1103/PhysRevB.87.155421.

[23] D. Chen and D. Sarid, Surface Science **329**, 206 (1995).

[24] C. Virojanadara and L. I. Johansson, Phys. Rev. B **71**, 195335 (2005).

[25] C. Virojanadara and L. Johansson, Surf. Sci. **600**, 436 (2006), ISSN 0039-6028, URL http://www.sciencedirect.com/science/article/B6TVX-4HR7442-1/2/05a1c4b33377586f1a1e98620e899fe7.

[26] A. Goldoni, R. Larciprete, C. Cepek, C. Masciovecchio, F. El Mellouhi, R. Hudej, M. Sancrotti, and G. Paolucci, Surf. Rev. Lett. **9**, 775 (2002).

[27] M. Pedio, F. Borgatti, A. Giglia, N. Mahne, S. Nannarone, S. Giovannini, C. Cepek, E. Magnano, G. Bertoni, E. Spiller, et al., Phys. Scr. **T115**, 695 (2005).

[28] L. I. Johansson, F. Owman, and P. Mårtensson, Phys. Rev. B **53**, 13793 (1996).

[29] L. S. O. Johansson, L. Duda, M. Laurenzis, M. Krieftewirth, and B. Reihl, Surf. Sci. **445**, 109 (2000), ISSN 0039-6028, URL http://www.sciencedirect.com/science/article/B6TVX-3Y9G7PX-S/2/2cb4b46bbd10e85f6c5e16f4a61965da.

[30] J. Furthmüller, F. Bechstedt, H. Hüsken, B. Schröter, and W. Richter, Phys. Rev. B **58**, 13712 (1998).

[31] J. R. Ahn, S. S. Lee, N. D. Kim, C. G. Hwang, J. H. Min, and J. W. Chung, Surf. Sci. **516**, L529 (2002), ISSN 0039-6028, URL http://www.sciencedirect.com/science/article/B6TVX-46DPFHG-4/2/8291505233c286dec25049f4e0674ab1.

[32] A. Goldoni, C. Cepek, M. D. Seta, J. Avila, M. Asensio, and M. Sancrotti, Surf. Sci. **454-456**, 514 (2000), ISSN 0039-6028, URL http://www.sciencedirect.com/science/article/pii/S0039602800002120.

[33] C. P. Cheng, T. W. Pi, C. P. Ouyang, and J. F. Wen, Journal Of Vacuum Science & Technology B **23**, 1018 (2005).

[34] J. M. Themlin, I. Forbeaux, V. Langlais, H. Belkhir, and J. M. Debever, Europhys. Lett. **39**, 61 (1997).

[35] P. Moriarty, M. D. Upward, A. W. Dunn, Y.-R. Ma, P. H. Beton, and D. Teehan, Phys. Rev. B **57**, 362 (1998).

[36] N. Yakovlev, X. Xianning, L. K. Ping, and X. Hai, Surf. Sci. **603**, 2263 (2009), ISSN 0039-6028, URL http://www.sciencedirect.com/science/article/B6TVX-4W7J0W1-1/2/9fe2e4711bf7f9946dd212a8c9e269ba.

[37] W. Chen, H. Xu, K. P. Loh, and A. T. S. Wee, Surf. Sci. **595**, 107 (2005), URL http://www.sciencedirect.com/science/article/B6TVX-4H0RYWR-1/2/63644875d28e40aa682ca2057dba0667.

[38] F. Amy, H. Enriquez, P. Soukiassian, P.-F. Storino, Y. J. Chabal, A. J. Mayne, G. Dujardin, Y. K. Hwu, and C. Brylinski, Phys. Rev. Lett. **86**, 4342 (2001).

[39] J. Schardt, J. Bernhardt, U. Starke, and K. Heinz, Phys. Rev. B **62**, 10335 (2000).

[40] V. A. Gasparov, M. Riehl-Chudoba, B. Schröter, and W. Richter, Europhys. Lett. **51**, 527 (2000), URL http://stacks.iop.org/0295-5075/51/i=5/a=527.

[41] I. F. Torrente, K. J. Franke, and J. I. Pascual, J. Phys.: Condens. Matter. **20**, 184001 (2008).

[42] F. C. Bocquet, Y. Ksari, Y. P. Lin, L. Porte, and J.-M. Themlin, Physical Review B **88**, 125421 (2013), URL http://link.aps.org/doi/10.1103/PhysRevB.88.125421.

[43] Y.-P. Lin, Y. Ksari, J. Prakash, L. Giovanelli, J.-C. Valmalette, and J.-M. Themlin, Carbon **73**, 216 (2014), ISSN 0008-6223, URL http://www.sciencedirect.com/science/article/pii/S0008622314001985.

[44] Y.-P. Lin, Y. Ksari, and J.-M. Themlin, Nano Research **8**, 839 (2015), ISSN 1998-0124, URL http://dx.doi.org/10.1007/s12274-014-0566-0.

[45] J. Ristein, S. Mammadov, and T. Seyller, Physical Review Letters **108**, 246104 (2012), URL http://link.aps.org/doi/10.1103/PhysRevLett.108.246104.

[46] S. Mammadov, J. Ristein, R. J. Koch, M. Ostler, C. Raidel, M. Wanke, R. Vasiliauskas, R. Yakimova, and T. Seyller, 2D Materials **1**, 035003 (2014), URL http://stacks.iop.org/2053-1583/1/i=3/a=035003.

[47] F. Bechstedt, *Principles of Surface Physics* (Springer, 2003).

[48] J.-M. Themlin, S. Bouzidi, F. Coletti, J.-M. Debever, G. Gensterblum, L.-M. Yu, J.-J. Pireaux, and P. A. Thiry, Phys. Rev. B **46**, 15602 (1992).
[49] A. Many, Y. Goldstein, and N. B. Grover, *Semiconductor Surfaces* (North-Holland Publishing Co., Amsterdam, 1965).
[50] T. R. Ohno, Y. Chen, S. E. Harvey, G. H. Kroll, J. H. Weaver, R. E. Haufler, and R. E. Smalley, Phys. Rev. B **44**, 13747 (1991).
[51] G. Gensterblum, K. Hevesi, B.-Y. Han, L.-M. Yu, J.-J. Pireaux, P. A. Thiry, R. Caudano, A.-A. Lucas, D. Bernaerts, S. Amelinckx, et al., Phys. Rev. B **50**, 11981 (1994).
[52] G. Cherkashinin, S. Krischok, M. Himmerlich, O. Ambacher, and J. A. Schaefer, J. Phys.: Condens. Matter **18**, 9841 (2006), URL `http://stacks.iop.org/0953-8984/18/i=43/a=006`.
[53] A. Brambilla, P. Sessi, L. Duò, M. Finazzi, J. Cabanillas-Gonzalez, H.-J. Egelhaaf, G. Lanzani, and F. Ciccacci, Surf. Sci. **601**, 4078 (2007), ISSN 0039-6028, eCOSS-24, Proceedings of the 24th European Conference on Surface Science, URL `http://www.sciencedirect.com/science/article/pii/S0039602807003500`.
[54] J. Y. Lee and M. H. Kang, Surf. Sci. **602**, 1408 (2008), ISSN 0039-6028, URL `http://www.sciencedirect.com/science/article/B6TVX-4RWBSW1-1/2/d9b19440581fb16a14dbbe35b79918cf`.
[55] J. Y. Lee and M. H. Kang, Phys. Rev. B **75**, 125305 (2007), URL `http://link.aps.org/doi/10.1103/PhysRevB.75.125305`.
[56] S. Gangopadhyay, R. Woolley, R. Danza, M. Phillips, K. Schulte, L. Wang, V. Dhanak, and P. Moriarty, Surf. Sci. **603**, 2896 (2009), ISSN 0039-6028, URL `http://www.sciencedirect.com/science/article/B6TVX-4WXHBRH-5/2/1cc5489830c48e12d505ebb02c0636da`.
[57] M. De Seta, D. Sanvitto, and F. Evangelisti, Phys. Rev. B **59**, 9878 (1999).
[58] D. Sánchez-Portal, E. Artacho, J. I. Pascual, J. Gómez-Herrero, R. M. Martin, and J. M. Soler, Surface Science **482-485, Part 1**, 39 (2001), ISSN 0039-6028, URL `http://www.sciencedirect.com/science/article/pii/S0039602800010086`.
[59] P. D. Godwin, S. D. Kenny, and R. Smith, Surf. Sci. **529**, 237 (2003), ISSN 0039-6028, URL `http://www.sciencedirect.com/science/article/B6TVX-47TWS85-1/2/9219e186fd0e967402f23ab10a495d0a`.
[60] S. Krummacher, M. Biermann, M. Neeb, A. Liebsch, and W. Eberhardt, Physical Review B **48**, 8424 (1993), URL `http://link.aps.org/doi/10.1103/PhysRevB.48.8424`.
[61] T. Liebsch, O. Plotzke, F. Heiser, U. Hergenhahn, O. Hemmers, R. Wehlitz, J. Viefhaus, B. Langer, S. B. Whitfield, and U. Becker, Physical Review A **52**, 457 (1995), URL `http://link.aps.org/doi/10.1103/PhysRevA.52.457`.
[62] A. Goldoni, C. Cepek, R. Larciprete, L. Sangaletti, S. Pagliara, G. Paolucci, and M. Sancrotti, Physical Review Letters **88**, 196102 (2002), URL `http://link.aps.org/doi/10.1103/PhysRevLett.88.196102`.
[63] E. Magnano, S. Vandré, C. Cepek, A. Goldoni, A. D. Laine, G. M. Curró, A. Santaniello, and M. Sancrotti, Surf. Sci. **377-379**, 1066 (1997), ISSN 0039-6028, european Conference on Surface Science, URL `http://www.sciencedirect.com/science/article/pii/S0039602897015471`.
[64] A. J. Maxwell, P. A. Brühwiler, A. Nilsson, N. Mårtensson, and P. Rudolf, Phys. Rev. B **49**, 10717 (1994).
[65] P. Rudolf, M. S. Golden, and P. A. Brühwiler, J. Electron Spectrosc. Relat. Phenom. **100**, 409 (1999), ISSN 0368-2048, URL `http://www.sciencedirect.com/science/article/pii/S0368204899000584`.
[66] N. Swami, H. He, and B. E. Koel, Phys. Rev. B **59**, 8283 (1999).
[67] M. Pedio, K. Hevesi, N. Zema, M. Capozi, P. Perfetti, R. Gouttebaron, J. J. Pireaux, R. Caudano, and P. Rudolf, Surf. Sci. **437**, 249 (1999), ISSN 0039-6028, URL `http://www.sciencedirect.com/science/article/pii/S0039602899007323`.
[68] A. Pesci, L. Ferrari, C. Comicioli, M. Pedio, C. Cepek, P. Schiavuta, M. Pivetta, and M. Sancrotti, Surf. Sci. **454-456**, 832 (2000), ISSN 0039-6028, URL `http://www.sciencedirect.com/science/article/pii/S0039602800000765`.
[69] A. J. Maxwell, P. A. Brühwiler, D. Arvanitis, J. Hasselström, M. K.-J. Johansson, and N. Mårtensson, Phys. Rev. B **57**, 7312 (1998).
[70] C. T. Tzeng, K. D. Tsuei, H. M. Cheng, and R. Y. Chu, J. Phys.: Condens. Matter **19**, 176009 (2007).
[71] G. Baffou, A. J. Mayne, G. Comtet, G. Dujardin, P. Sonnet, and L. Stauffer, Applied Physics Letters, 073101, **91** (2007).
[72] O. Boudrioua, H. Yang, P. Sonnet, L. Stauffer, A. J. Mayne, G. Comtet, G. Dujardin, Y. Kuk, S. Nagarajan, A. Gourdon, E. Duverger, Phys.Rev.B, 035423 **85** (2012).
[73] J. E. Grose, E. S. Tam, C. Timm, M. Scheloske, B. Ulgut, J. J. Parks, H. D. Abruna, W. Harneit, and D. C. Ralph, Nature Materials **7**, 884 (2008), ISSN 1476-1122.
[74] Remarkably, adding a further component did not improve the fit appreciably, suggesting the presence of several nonequivalent atomic sites.
[75] On Si(100)-(2x1), it has been shown that the smallest separation between adjacent C_{60} is 11.5 Å, much larger than 10.05 Å, the van der Waals separation in a C_{60} pair[11].
[76] T. Ovramenko, PhD Thesis, University of Paris Sud, Orsay (2012).
[77] Si(111)-(2×1) presents a surface band gap of 0.3 eV, while Si(111)-(7×7) is metallic.
[78] In Sec.III, we have warned that a broad SiC-derived peak located around 3 eV could affect the lineshape in this region. However, it should affect equally both HOMO and HOMO-1, while the observed broadening is limited to the shallowest.